MICROSCALE BACKGROUND-ORIENTED SCHLIEREN FOR FLOW VISUALIZATION AND QUANTITATIVE ANALYSIS IN A MICROFLUIDIC OSCILLATOR

C.-l. SUN[1,c], T.-h. HSIAO[2]

[1]Department of Mechanical Engineering National Taiwan University, Taipei City, Taiwan
[2]Department of Mechanical Engineering National Taiwan University of Science and Technology, Taipei City, Taiwan

[c]Corresponding author: Tel.: +886-2-3366-1505; Fax: +886-2363-1755; Email: clsun@ntu.edu.tw

KEYWORDS:
Main subjects: mass transport phenomena, flow visualization, quantitative analysis
Fluid: microscale mixing
Visualization method(s): microscale background-oriented schlieren
Other keywords: microfluidic oscillator, refractive index gradient

ABSTRACT: In this study, we employ the microscale Background-Oriented Schlieren (μBOS) to facilitate measurement of inhomogeneities in a microfluidic oscillator. A photomask randomly patterned with dots of 4 μm in diameter is designed and placed in the background of the test volume. When miscible fluids with different refractive indices are mixed in microfluidics, resultant inhomogeneities lead to gradient of refractive index and light is deflected to cause dot shifts in the acquired image. By comparing the distorted image and the original background, dot displacements can be determined from ImageJ [1] with Particle Image Velocimetry (PIV) plugin. A calibration procedure is first conducted by mixing dilute aqueous ethanol and water in a T-microchannel to obtain the relation between concentration gradient and dot displacement. The sensitivity of our μBOS system is constrained by the smallest displacement of dot that is detectable and found to be corresponded to $\nabla C \sim 3.4 \times 10^{-6}$ μm^{-1}. Based on the calibration curve, μBOS image can be analyzed to quantify the inhomogeneities during the mixing process in a microfluidic oscillator. Compared to micro-schlieren and fluorescence techniques, we find that μBOS is able to reveal the detailed mass transport that is hidden from other flow visualization methods. Regions with large concentration gradient ($\partial C/\partial x$) are identified near the concave surface, indicating that part of the low-concentration fluid is stretched by the dominant vortex. Moreover, the magnitude of $\partial C/\partial y$ is relatively high inside the two vortices, because fluids of different concentration are entrained by the vortices. These entrainments promote the transverse mass transport and enhance the mixing process in the microfluidic oscillator.

INTRODUCTION: Benefiting from reduced consumption of reagent, cost saving, rapid response and compactness, microfluidic platform emerges as a promising platform for Micro-Total-Analysis-System (μTAS). To take full advantages of microfluidics, understanding the complex transport phenomena involved is key to achieve the optimal design for different functionalities. Among others, micro-Particle Imaging Velocimetry (μPIV) [2, 3] and fluorescence detection [4] are some of the most commonly used methods for quantitative analysis. Yet, these approaches have limitation in configurations to prevent them from elucidating the three-dimensionality of flow in microfluidics. In our previous study [5], we have developed a micro-schlieren system to address this issue. Although the micro-schlieren technique was proven to be quite successful in providing spatially-resolved, noninvasive, full-field transient measurement, its quantitative analysis was somehow constrained by the orientation of the knife-edge. To overcome this issue, we propose to use the μBOS approach instead. Simpler than the conventional schlieren setup, Background-Oriented Schlieren (BOS) system does not require a knife-edge to block a portion of the refractive light. Rather, the optical inhomogenerities in the evaluation zone is exhibited by comparing the distorted image and the original background. Once the displacement vectors of distortions are computed, BOS is able to offer information on gradients of refractive index in all directions simultaneously.

Meier [6] pioneered the BOS technique to analyze a supersonic jet, helium concentration in a gas plume, vortex shedding behind a cylinder, and the density gradient field of a gun shot. Using a deliberate background with sufficient optical contrast, existing evaluation algorithms for Particle Imaging Velocimetry (PIV) were employed to quantify the shifts in image details that were proportional to the light deflection by the field gradients. A similar technique, called 'synthetic schlieren,' was proposed by Dalziel, et al. [7]. Dalziel, et al. [7] used three different background patterns, parallel lines, regular dot arrays, and random dots, to realize qualitative visualizations of density fluctuations and obtain quantitative whole-field density measurements in two-dimensional density-stratified flows. The application of their technique was demonstrated in an internal wave field produced by an oscillating cylinder. Moreover,

Richard and Raffel [8] suggested that the BOS technique provide great flexibility to yield useful quantitative information for onsite aerodynamic study. Using the natural background, vortex formation from the blade tips of helicopters in flight were visualized and quantified. Other applications, such as studies of shock wave in supersonic flow [9, 10] and plume [11] were also demonstrated. The 'microscale synthetic schlieren' was first demonstrated by Yick, et al. [12, 13] using a stereo microscope with a 0.5X objective and a random pattern of 35 μm dots. For a sphere settling in salt stratification, Yick, et al. [14] documented the density fields and found a settling sphere drew lighter fluid downwards to form a density wake at small Reynolds numbers. Later, another configuration of μBOS was proposed by Schröder, et al. [15] using a long-distance microscope and a digital mirror device for synchronized projection of random dots. Schröder, et al. [15] integrated the displacement vector field along different viewing path in order to reconstruct the density fields inside a micro nozzle plumes with tomographic algorithm. Detection of very low density gradient was achieved and a sensitivity of 10^{-10} μm^{-1} was reached for refractive index gradient.

As mentioned in previous literatures, μBOS technique has shown great potential in elucidating fluid dynamics that involved the variation of refractive index. Herein, we demonstrate the utilization of μBOS to study the mixing process in a microfluidic oscillator. A photomask randomly patterned with dots of 4 mm in diameter is designed to serve as the background. Starting with a calibration procedure in a T-microchannel, we develop the quantitative methodology to measure the inhomogeneities in more complex microfluidics. The outcome offers a valuable insight into the microscale mass transport phenomena that other methods fail to deliver.

EXPERIMENTAL SETUP: The experimental schematic of the μBOS setup is illustrated in Fig. 1. The μBOS system consists of an inverted microscope (DM-IRM, Leica) with a 10X objective (N Plan L, Leica, NA = 0.25), a high performance monochrome CCD camera (CoolSNAP EZ, Photometrics), and a personal computer equipped with image acquisition software (RS image 1.9.2, Roper scientific) and image analysis software (ImageJ [1] with PIV plugin). For illumination, a 100 W halogen lamp is arranged in backlighting configuration. A random-dot photomask is placed between the microfluidic device and the light source to serve as the background. The acquired image has 1392 x 1040 pixels, and the spatial scale is approximately 1 μm/pixel under our magnification. During experiments, pure water and dilute aqueous ethanol (3% of ethanol content by weight) are chosen as the working fluids due to the linear correlation between refractive index and concentration within this range [16]. A syringe pump (kds210, KD Scientific) is employed to deliver the working fluids to the microchannel. In this study, two PDMS (Polydimethylsiloxane) microfluidic devices are tested: a T-microchannel for calibration purpose and a microfluidic oscillator. Standard SU8 (SU-8 2150, MicroChem) molding method are used to fabricate all PDMS devices. The T-microchannel consists of two 90 μm wide and 2500 μm long fluid feed ducts and a 360 μm wide, 3000 μm long exit channel. The microfluidic oscillator comprises a T-shaped confluence region, a divenging section with a concave obstacle, and an exit channel. Detail dimensions of the microfluidic oscillator A450S can be found in [17]. The depth of both devices is 170.5 μm. The distance between the dot pattern and the device directly affect the sensitivity of our μBOS system [9]. Although setting the device and the random-dot background further apart enhances the sensitivity, the small depth of field for microscope makes it difficult to attain a clear image of the test volume and the background at the same time. To compromise with these conflicting demands, the dot pattern is kept 950 μm above the device in this study.

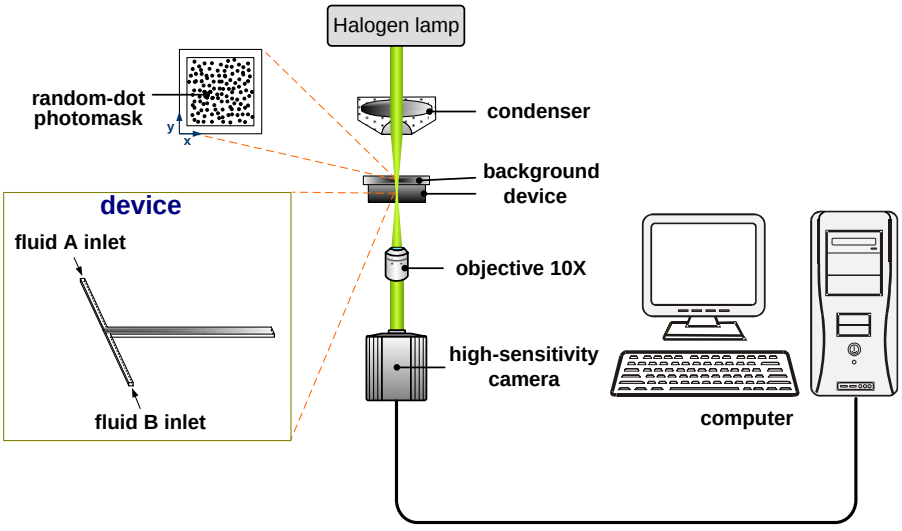

Fig. 1 Experimental schematic of the μBOS system for quantitative analysis

The random-dot design is vital to the correct estimation of image displacement. Herein, we make a chrome-on-glass photomask to serve as the random-dot background. A MATLAB (Mathworks) program is written to follow the flowchart outlined in Fig. 2 for the design of the random-dot pattern. First, we divide the evaluation zone into M×N interrogation cells, and each cell is further subdivided into 4×4 matrix. Since PIV processing is optimized when each interrogation cell contains seven seeding particles [18], seven elements out of the total 16 in the 4×4 matrix are randomly picked and assigned the value 1. Other elements in the matrix remain to contain value 0. The value of 1 indicates that a particle is resided within this element. This process is repeated M×N times for every interrogation cells in the evaluation zone. The indices (i, j) of the non-zero elements are then transformed to the actual coordinate (x_i, y_j). The data of these coordinates are imported to AutoLISP (Autodesk) in order to produce the final AutoCAD file. While the spatial resolution of the mask writer defines the minimum dot pitch and diameter, the optimal diameter of the dots depends on the magnification, the actual dimension of the evaluation zone, and the resolution of CCD camera. In this study, we select a dot diameter of 4 μm and all dots are at least 4 μm away from each other.

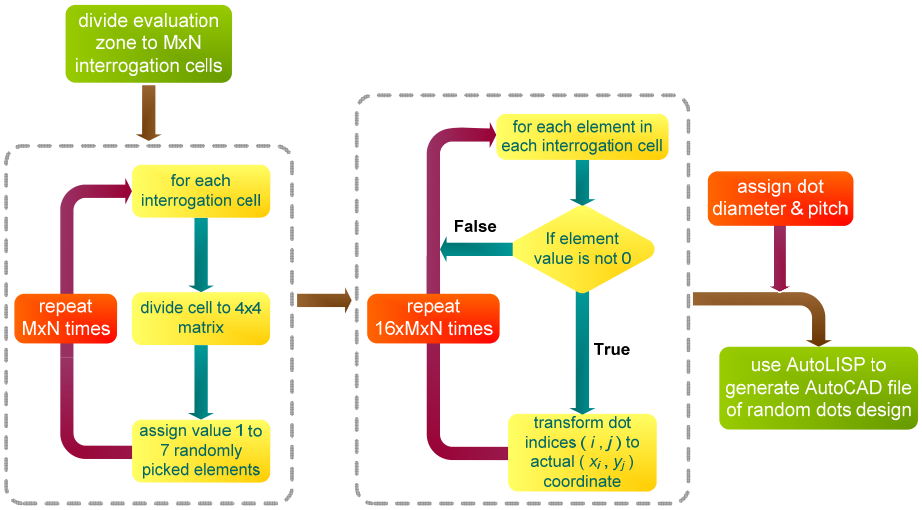

Fig. 2 Design flowchart of the random-dot background

METHODOLOGY: The μBOS technique relies on the comparison between the distorted image and the original background to measure the optical inhomogeneities presented in the test volume. Fundamentally, the level of distortion is proportional to the refractive index gradient of the medium. To implement quantitative analysis of μBOS, a calibration procedure using simple geometry microchannel with the known should be carried out first. The proposed methodology flowchart is depicted in Fig. 3.

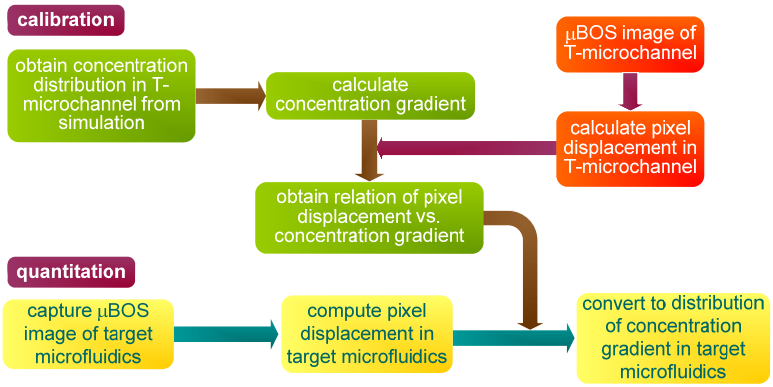

Fig. 3 Methodology flowchart of μBOS quantitative analysis

The calibration procedure is carried out by mixing dilute aqueous ethanol and water in a T-microchannel to obtain the relation between pixel displacement of dots and concentration gradient. Prior to the mixing process, the reference image is taken when the T-microchannel is filled with pure water. The cross-correlation algorithm of PIV is employed to determine the pixel displacement from the μBOS and reference image pair. On the other hand, we are able to estimate the concentration profile in the T-microchannel from numerical simulation and hence calculate its

corresponding concentration gradient across the interface during mixing. Therefore, comparison of the pixel displacements to the concentration gradient profile provides the correlations between these two quantities. Theoretically, pixel displacement of distorted image is proportional to the refractive index gradient. In the concentration range we use here, refractive index of the working fluid varies linearly with its composition. Hence, the calibration curve of concentration gradient and pixel displacement should be a straight line. For quantitative analysis, the process is reversed and distribution of concentration gradient is known once the μBOS and reference images are captured in the target microfluidics.

The sensitivity of μBOS depends on the minimum pixel displacement that can be detected by the PIV evaluation. Influential factors include optical arrangement of the μBOS system, size of interrogation cells, dot diameter, dot density, and displacement gradients. By generating an artificial image shift, we find that ImageJ [1] with PIV plugin is able to resolve a displacement down to 0.0023 pixel.

CALIBRATION: Following the procedure of methodology, calibration process is performed by mixing dilute aqueous ethanol (mass fraction w = 3%, normalized concentration C = 1) and pure water (w = 0, C = 0) in the 170.5 μm deep T-microchannel. The reference image is taken when the T-microchannel is full of pure water so that a constant refractive index field is maintained. The μBOS results are shown in Fig. 4 at a Reynolds number of 1. As shown in Fig.4, the vectors and magnitudes of the pixel displacement imply the directions and levels of distortion. The light is bent toward region with higher concentration and largest pixel displacement is found at the interface of mixing. As shown in Fig. 4 (b), the contour of displacement magnitude depicts a broadening and gradually fading band in the streamwise direction because of mass diffusion and dispersion across the interface. Poor results are produced at the channel intersection however. This is because the abrupt change in refractive index causes a natural shadow, blurring the μBOS image and leading to errors in PIV evaluation.

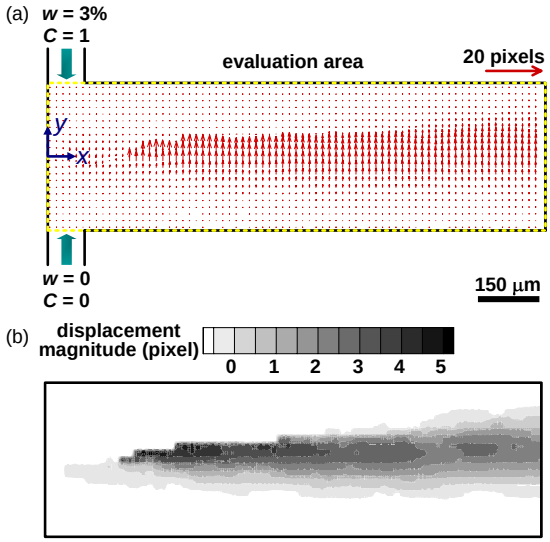

Fig. 4 (a) Displacement field, (b) contour of displacement magnitude in the T-microchannel

To obtain the calibration curve, a software package based on finite volume approach, CFD-ACE+ [19], is employed to predict the concentration profile in the T-microchannel. Assuming steady, laminar, and incompressible, a three-dimensional model is constructed for the T-microchannel and computed to obtain the normalized concentration distribution. Then, we use the central differencing scheme to calculate the concentration gradients with respect to the cross-stream coordinate $\partial C/\partial y$ for each xy plane, and take the average in the z direction. Fig. 5 (a) exhibits the comparison of the concentration gradient profile and the pixel displacement along the centerline of the T-microchannel (y = 0). For x < 300 μm, a large discrapancy exists due to the shadow blurring effect discussed earlier. Therefore, we choose the results from 500 μm < x < 1500 μm to plot the calibration curve, as shown in Fig. 5 (b). A linear relation is found between the concentration gradient and the pixel displacement, and the equation obtained from the least squares fitting is also displayed in Fig. 5 (b). This mathemtaical relation can be used to evaluate concentration gradient in more complex microfluidics once their μBOS images are captured. The error of $\partial C/\partial y$ is ±5.0%, and the sensitivity limit of our μBOS is $\nabla C \sim 3.4 \times 10^{-6}$ μm^{-1} (or $\nabla n \sim 2.32 \times 10^{-7}$ μm^{-1}) correspondingly.

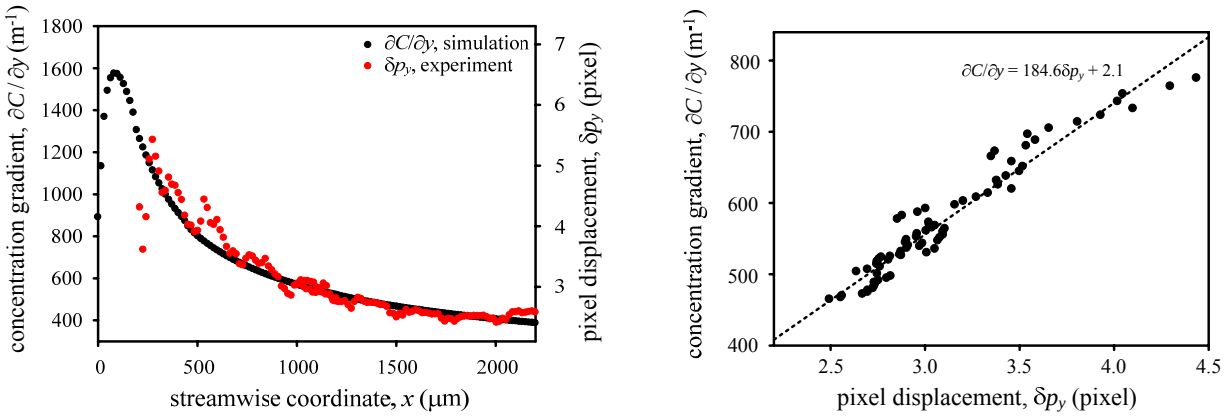

Fig. 5 (a) Comparison of concentration gradient and pixel displacement, (b) calibration curve of μBOS

RESULTS: Mixing in microfluidic oscillator A450S [17] is utilized to demonstrate flow visualization and quantitative analysis of the μBOS system. The microfluidic oscillator consists of a jet impinging onto a concave surface in order to induce the Coandă effect and the Görtler instability to promote mixing [17].

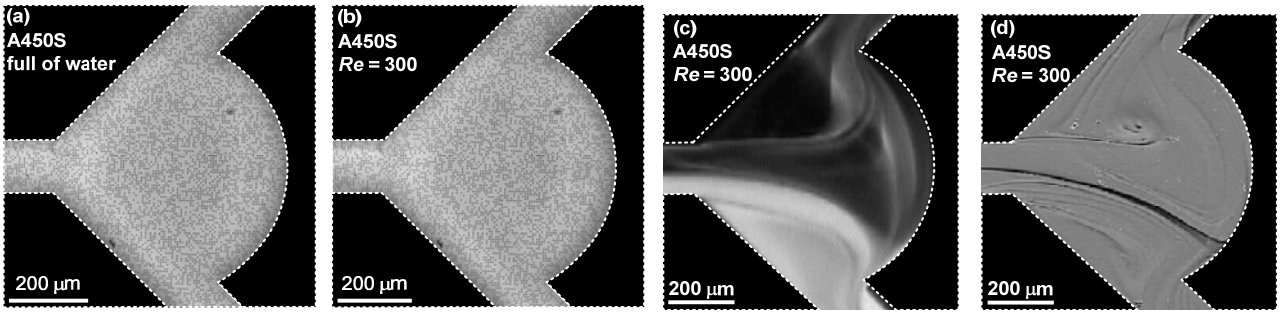

Fig. 6 (a) The reference image, (b) the μBOS image (c) the fluorescence image [17], (d) micro-schlieren result [5] in microfluidic oscillator A450S during mixing

The reference and the distorted images of microfluidic oscillator A450S are displayed in Fig. 6 (a) and Fig (b). For reference, the fluorescence and micro-schlieren images from previous studies [5, 17] are exhibited in Fig. 6 (c) and Fig. (d). The reference background is captured when the microfluidic oscillator is completely filled with pure water, i.e. no refractive index gradient is present in the test volume. On the other hand, the μBOS image is taken when dilute aqueous ethanol of w = 3% and pure water are supplied to the microfluidic oscillator and mixed at a Reynolds number of 300. After data processing, the results are shown in Fig. 7.

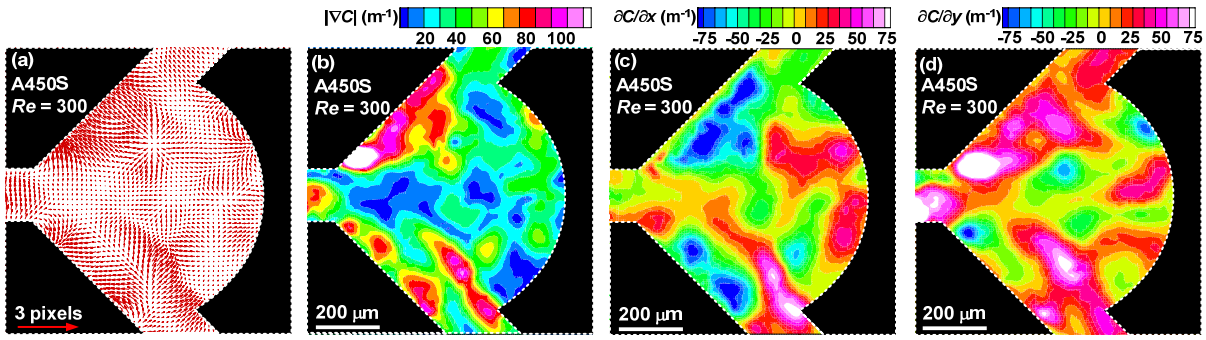

Fig. 7 (a) Displacement field, (b) contour of the magnitude of concentration gradient, (c), contour of $\partial C/\partial x$ (d) contour of $\partial C/\partial y$ in microfluidic oscillator A450S during mixing

By Comparing Fig. 7 (a) to Fig. 6 (d), we find that the locations of the vortex centers either correspond to a source point or lie on a positive bifurcation line where vectors of pixel displacement sprout. Since the light is always

deflected in the direction of increasing refractive index, a source or positive bifurcation line indicates a local region of relatively low concentration, and a sink or negative bifurcation line refers to a local region of relatively high concentration. Regions of large magnitude of displacement are found along the boundary of the two vortices and inside the larger vortex near the upper sidewall, suggesting that the vortices help to entrain fluids of different concentration and play an important role in mixing. To understand the detailed mass transport, Fig. 7 (c) and Fig. 7 (d) show the concentration gradients of $\partial C/\partial x$ and $\partial C/\partial y$, correspondingly. In Fig. 7 (c), region near the concave surface also exhibits large value of $\partial C/\partial x$. This agrees with Fig. 6 (c) that filament of fluorescence (associated with low-concentration fluid) is stretched by the large vortex. Fig. 7 (d) indicates that strong transverse transport occurs inside the microfluidic oscillator. Concentration gradient with respect to the cross-stream direction $\partial C/\partial y$ can easily exceed 60 m^{-1} near the sidewalls. Unlike micro-schlieren which is constrained by the orientation of knife-edge, μBOS is able to provide gradient information in all directions simultaneously.

Herein, we demonstrate the use of μBOS to a microfluidic oscillator for flow visualization and quantitative analysis. Using the random-dot photomask as the background, μBOS proves to offer an insight to unique characteristics for mixing process in a microfluidic oscillator at high Reynolds number. Moreover, this technique can be applied to other scalar quantitations that are associated with the variation of refractive index in the future.

CONCLUSION: In this study, we demonstrate the flow visualization and quantitative analysis for the mixing process in a microfluidic oscillator using μBOS technique. A random-dot photomask is designed and implemented as the background for the PIV evaluation. When inhomogeneities are present in the test volume, gradient of refractive index leads to light deflection that results in dot shifts. From the directions and magnitudes of these displacement vectors, we are able to measure gradients of refractive index in both streamwise and cross-stream directions simultaneously. Once the calibration procedure is performed by mixing in a T-microchannel, the relation between concentration gradient and pixel displacement can be used to determine the concentration gradient field in the microfluidic oscillator from its μBOS image. The μBOS proves to be a robust and powerful tool in distinguishing unique mass transport phenomena during the mixing process in the microfluidic oscillator at high Reynolds number.

In the future, the present technique shows great potential in quantifying other scalar fields that are associated with the variation in refractive index.

ACKNOWLEDGEMENT: This work is supported by the National Science Council of Taiwan under grant number NSC 100-2221-E-002-251.

References

1. Abramoff M.D. et al *Image Processing with ImageJ.* Biophotonics Int. 2004, **11** (7), p. 36-42
2. Santiago J.G. et al *A Particle Image Velocimetry System for Microfluidics.* Experiments in Fluids 1998, **25** (4), p. 316-319
3. Meinhart C.D. and Zhang H.S. *The Flow Structure Inside a Microfabricated Inkjet Printhead.* Journal of Microelectromechanical Systems 2000, **9** (1), p. 67-75
4. Roulet J.-C. et al *Performance of an Integrated Microoptical System for Fluorescence Detection in Microfluidic Systems.* Anal. Chem. 2002, **74** (14), p. 3400-3407
5. Hsiao T.-h. and Sun C.-l. *Application of Micro-Schlieren Technique to Quantitative Analysis of Mass Transport in a Micromixer*. *Proc. of AJK*, Hamamatsu, Japan, 2011
6. Meier G.E.A. *Computerized Background-Oriented Schlieren.* Exp. Fluids 2002, **33** (1), p. 181-187
7. Dalziel S.B. et al *Whole-Field Density Measurements by 'Synthetic Schlieren'.* Exp. Fluids 2000, **28** (4), p. 322-335
8. Richard H. and Raffel M. *Principle and Applications of the Background Oriented Schlieren (BOS) Method.* Meas. Sci. Technol. 2001, **12** (9), p. 1576
9. Venkatakrishnan L. and Meier G.E.A. *Density Measurements Using the Background Oriented Schlieren Technique.* Exp. Fluids 2004, **37** (2), p. 237-247
10. Ramanah D. et al *Background Oriented Schlieren for Flow Visualisation in Hypersonic Impulse Facilities.* Shock Wav. 2007, **17** (1), p. 65-70
11. Settles G.S. *Schlieren and Showdowgraph Techniques*. 2nd ed, Springer New York, 2001
12. Yick K.Y. et al *Enhanced drag of a sphere settling in a stratified fluid at small Reynolds numbers.* Journal of Fluid Mechanics 2009, **632**, p. 49-68
13. Yick K.-Y. et al *Microscale synthetic schlieren.* Experiments in Fluids 2007, **42** (1), p. 41-48
14. Yick K.Y. et al *Microscale Synthetic Schlieren.* Exp. Fluids 2007, **42** (1), p. 41-48

15. Schröder A. et al *Measurements of density fields in micro nozzle plumes in vacuum by using an enhanced tomographic background oriented schlieren (BOS) technique*. *Proc. of The 9th International Symposium on Measurement Technology and Intelligent Instruments*, Saint-Petersburg, Russia, 2009
16. Scott T.A. *Refractive Index of Ethanol–Water Mixtures and Density and Refractive Index of Ethanol–Water–Ethyl Ether Mixtures.* J. Phys. Chem. 1946, **50** (5), p. 406-412
17. Sun C.-l. and Sun C.-Y. *Effective Mixing in a Microfluidic Oscillator Using an Impinging Jet on a Concave Surface.* Microsys. Technol. 2011, **17** (5), p. 911-922
18. Raffel M. et al *Particle Image Velocimetry: A Practical Guide*. 2nd ed, Springer, Heidelberg, 2007
19. *CFD-ACE+ V2007.2 User Manual*. 2007, ESI CFD: Huntsville, AL.